tvst

DOI: 10.1167/tvst.6.5.11

Article

Driving with Hemianopia V: Do Individuals with Hemianopia Spontaneously Adapt Their Gaze Scanning to Differing Hazard Detection Demands?

Concetta F. Alberti[1], Robert B. Goldstein[2], Eli Peli[2], and Alex R. Bowers[2]

[1] Department of Psychology, College of Science, Northeastern University, Boston, MA, USA
[2] Schepens Eye Research Institute, Massachusetts Eye and Ear, Harvard Medical School, Boston, MA, USA

Correspondence: Alex Bowers, Schepens Eye Research Institute, 20 Staniford Street, Boston MA 02114, USA. e-mail: alex_bowers@meei.harvard.edu

Received: 24 March 2017
Accepted: 06 September 2017
Published: 23 October 2017

Keywords: head movements; eye movements; gaze; detection; adaptation; hemianopia; rehabilitation

Citation: Alberti CF, Goldstein RB, Peli E, Bowers AR. Driving with hemianopia V: do individuals with hemianopia spontaneously adapt their gaze scanning to differing hazard detection demands? Trans Vis Sci Tech. 2017;6(5):11, doi: 10.1167/tvst.6.5.11

Purpose: We investigated whether people with homonymous hemianopia (HH) were able to spontaneously (without training or instructions) adapt their blind-side scan magnitudes in response to differing scanning requirements for detection of pedestrians in a driving simulator when differing cues about pedestrian eccentricities and movement behaviors were available in the seeing hemifield.

Methods: Twelve HH participants completed two sessions in a driving simulator pressing the horn when they detected a pedestrian. Stationary pedestrians outside the driving lane were presented in one session and approaching pedestrians on a collision course in the other. Gaze data were analyzed for pedestrians initially appearing at approximately 14° in the blind hemifield. No instructions were given regarding scanning.

Results: After appearing, the stationary pedestrians' eccentricity increased rapidly to a median of 31° after 2.5 seconds, requiring increasingly larger blind-side gaze scans for detection, while the approaching pedestrians' eccentricity remained constant at approximately 14°, requiring a more moderate scan (~14°) for detection. Although median scan magnitudes did not differ between the two conditions (approaching: 14° [IQR 9°–15°]; stationary: 13° [IQR 9°–20°]; $P = 0.43$), three participants showed evidence of adapting (increasing) their blind-side scan magnitudes in the stationary condition.

Conclusions: Three participants (25%) appeared to be able to apply voluntary cognitive control to modify their blind-side gaze scanning in response to the differing scanning requirements of the two conditions without explicit training.

Translational Relevance: Our results suggest that only a minority of people with hemianopia are likely to be able to *spontaneously* adapt their blind-side scanning in response to rapidly changing and unpredictable situations in on-road driving.

Introduction

Homonymous hemianopia (HH) is the loss of half the field of vision on the same side in both eyes. It is caused by lesions in the postchiasmal visual pathways, primarily due to strokes and, to a lesser extent, trauma and tumors.[1] People with HH may compensate for their hemifield loss by scanning using eye and/or head movements toward the blind hemifield. However, there is accumulating evidence[2] that many do not compensate well leading to impaired hazard detection in simulated driving,[3–8] in on-road driving,[9] and in walking tasks.[10]

In order to see an object in the blind hemifield, people with complete HH need to scan at least as far into the blind hemifield as the location of the object. However, they receive no visual cues from peripheral vision as to when to scan or how far to scan into the blind hemifield. People with HH are usually aware of their visual field loss (unless they have spatial neglect) and could use voluntary, cognitive control to guide their blind-side scanning. For example, patients with HH may be trained or told to scan to the blind side in order to detect potential hazards.[11] However, relatively little is known about the extent to which people with HH use such strategies in real world situations

(e.g., driving[2]) or whether they are able to adapt their scanning patterns in response to differing conditions (e.g., a busy city-center street with frequent hazards versus a quiet rural road with infrequent hazards).

Only a limited number of studies have addressed the question of whether people with HH adapt their scanning strategies. A recent study using a gaze-contingent simulation of HH concluded that efficient search strategies were not spontaneously adopted by the majority of participants; however, a minority (4/20) did modify their search strategy in response to changing task demands. In general, a strategy of searching the seeing side before the blind side was adopted both for difficult search tasks in which each item needed to be viewed in a serial fashion as well as easier tasks in which the target was clearly visible in the periphery and a large saccade toward the blind side would have been the more efficient strategy. Only four participants modified their search to start from the blind field when the task was easy. In another study, Schuett et al.[12] reported that normally sighted participants with simulated HH became more efficient at a dot-counting task (an irregular array of dots) and a reading task after a short period of practice (~15 minutes) on each of the tasks. However, in follow-up studies they found no evidence of transfer of learning (modification of gaze behaviors) between the two tasks, either for simulated HH[13] or real HH[13] (i.e., participants who practiced the dot-couting task did not demonstrate improvements on the reading task and vice versa).

In a study involving detection of peripherally presented moving basketballs within a virtual environment, participants with HH scanned less extensively in the horizontal plane and spent more time looking toward the ground when performing the task while walking than when seated.[10] Thus, when walking, it appears that they modified their gaze behaviors in favor of walking, at the expense of peripheral target detection. In a driving simulator study[3] involving detection of stationary pedestrians on the blind and seeing sides, no improvement in blind-side detection rates was found between two simulator sessions, approximately 1 week apart. These results suggested that no learning had occurred, despite 60 minutes of test drives at each session. Moreover, information was available in the seeing hemifield about pedestrian eccentricity, which could have been used as a guide for the scanning behaviors that were needed for detection of blind-side pedestrians. However, gaze movements were not recorded so it was unknown whether there were any changes in gaze behaviors.

In this paper, we report an analysis of gaze behaviors from a driving simulator study[5] in which we evaluated detection performance of people with HH for pedestrians that were stationary to the side of the driving lane and pedestrians that approached the driving lane, walking or running on a collision course (detection rates and reaction time results were reported previously[5]). The scanning requirements for successful detection of blind-side pedestrians differed for the two pedestrian conditions, providing an opportunity to examine whether participants adapted their scanning behaviors. In the stationary condition the pedestrians did not move after appearing.[3,5] Thus, their eccentricity increased rapidly as the car progressed, moving them farther into the blind hemifield, requiring increasingly larger gaze movements for detection. On the other hand, in the approaching condition, the pedestrians were on a collision course,[5,14] so their eccentricity remained approximately constant as the car progressed. Thus, the magnitude of the gaze scan needed for detection would also have remained approximately constant, and smaller than the gaze scan needed in the stationary condition.

Herein, we address two main questions: (1) did participants with HH adapt their blind-side scan magnitudes (without training or instructions) to match the differing scanning requirements (pedestrian eccentricities) for successful blind-side detection in the stationary and approaching conditions; and (2) were the previously reported[5] differences in blind-side detection rates between the two conditions accounted for by differences in the scanning requirements? We quantified the magnitudes of scans after the appearance of pedestrians in the blind hemifield and tested the hypothesis that blind-side scans would be larger in the stationary than the approaching condition. We expected to find greater evidence of within-session learning in the stationary condition (where scanning requirements were higher) than in the approaching condition. In addition, we tested the hypothesis that more time would be available after the pedestrian appearance for a moderate-sized gaze scan to reach the pedestrian in the approaching than the stationary condition, resulting in better detection rates but longer response times.

Methods

The study followed the tenets of the Declaration of Helsinki and was approved by the institutional review board at the Schepens Eye Research Institute.

Participants

The study was completed by 12 individuals with HH, as detailed previously.[5] All participants met the following inclusion criteria: (1) complete HH, as measured with a kinetic V4e target in a Goldmann perimeter; (2) no visual neglect (Bells test[15] and Schenkenberg line bisection test[16]; (3) no significant cognitive decline (Mini-Mental State Examination test[17] $\geq$ 24); (4) visual acuity of at least 20/40 in each eye with the habitual correction; (5) no physical impairment that could prevent the use of the standard vehicle controls (gas and brake pedals, steering wheel and horn); and (6) prior driving experience. Data presented in this paper were collected at the same time as the data previously reported[5] for these 12 participants with HH.

Apparatus

The driving simulator (LE-1500; FAAC Corp., Ann Arbor, MI) was comprised of five, 42-inch liquid-crystal display (LCD) monitors (LG M4212C-BA, native resolution of 1366 $\times$ 768 pixels; LG Electronics, Seoul, South Korea) providing a 225° horizontal field of view. The central screen (64° horizontal) provided the view through the windshield while the flanking and lateral screens provided the view from the lateral windows. The rear- and side-view mirrors were inset on the LCD monitors simulating the positions in a real car. The simulator included a motion seat with three degrees of freedom, a force-feedback steering wheel, a dashboard with the speedometer and other instrument displays, and all the usual controls found in an automatic transmission car. The simulated drives took place in a 1600 $\times$ 800-m virtual world.

Events in the virtual world were programmed through a scenario development toolbox (FAAC Corp.) that rendered the movement of pedestrians and vehicles dependent on the location of the participant's vehicle within the world. Data from the simulator stream (including the location and status of all programmed objects and the driver's car in the virtual world) were continuously recorded at 30 Hz. A Smart Eye remote six-camera infrared eye and head tracking system (Pro 5.4; Smart Eye, Gothenburg, Sweden) was used to track gaze at 60 Hz. This system enabled tracking across the full width of the field of view of the simulator with an accuracy of 2° across the central screen where the pedestrians appeared. Custom-written software was used to synchronize the 60-Hz Smart Eye data stream with the 30-Hz simulator data stream and the virtual world coordinate system.

Research Procedures and Detection Task

Participants completed two driving simulator sessions on separate days ($\sim$1 week apart), one with stationary and one with approaching pedestrians in counterbalanced order.[5] After practice drives that provided acclimation to the driving simulator and the detection task, a five-point calibration of the gaze tracker across the central driving simulator screen was performed. Participants then completed a total of approximately 60 minutes of experimental data collection in which they performed the pedestrian detection task while driving along predetermined routes in city and rural environments. Data collection was split into five test drives, each lasting approximately 10 to 12 minutes with short breaks between when needed (for many participants it would have been too tiring to complete 60 minutes of driving without a break).

Life-size pedestrian figures were scripted to appear on the central screen every 15 to 60 seconds, either on the right or left of the road at small ($\sim$4°) or large ($\sim$14°) eccentricities with respect to the center of the travel lane.[5] However, the actual eccentricities experienced by each participant varied depending on the speed and the position of the virtual vehicle within the travel lane. Each test drive contained an equal number of pedestrians at each eccentricity on the left and right sides. The pedestrians appeared at a distance of 67 m from the driver's car on city roads and 134 m on rural undivided highways, equivalent to approximately 5 seconds when traveling at 30 and 60 mph (the posted speed), respectively. The pedestrians initially subtended 1.7° vertically in city drives and half that in rural highway drives.

After appearing, pedestrians were either stationary in their initial position as the participant's car approached (stationary condition) or walked/ran toward the road as if to cross the car's trajectory (approaching condition). It was the same pedestrian figure for the stationary and approaching conditions; the only difference was whether the pedestrian remained stationary or walked/ran. In the approaching condition, small eccentricities ($\pm$4°) represented hazards approaching from an adjacent lane, or the sidewalk beside the participant's lane, while larger eccentricities ($\pm$14°) represented hazards approaching more quickly and from a greater distance (e.g., a jogger or a bicyclist approaching from the opposite sidewalk on a road with 2 lanes in each direction).

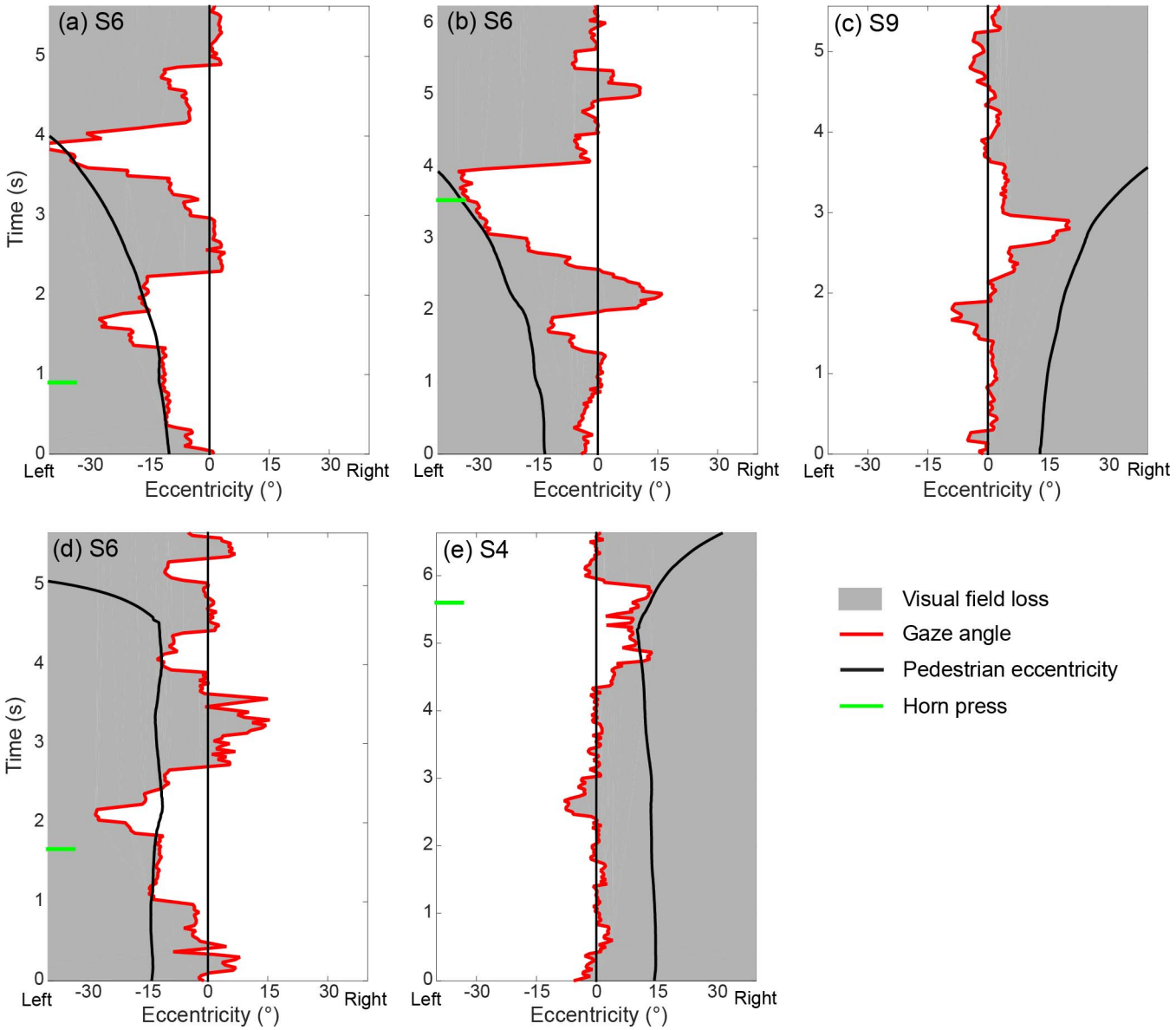

Figure 1. Plots for individual participants of lateral gaze eccentricity (*thick red line*) and pedestrian eccentricity (*thick black line*) with respect to car heading direction for pedestrians initially appearing at approximately 14° in the blind hemifield: (a) a stationary pedestrian detected less than 1 second after appearance by participant S6 with left hemianopia following a scan of approximately 13°; (b) a stationary pedestrian detected approximately 3 seconds after appearance by S6 following a large scan of approximately 28°; (c) a stationary pedestrian not detected (missed response) by participant S9 with right hemianopia despite a scan of approximately 20°; (d) an approaching pedestrian detected approximately 1 second after appearance by participant S6 following a scan of approximately 15°; and (e) an approaching pedestrian detected very late, approximately 4.7 seconds after appearance, by participant S4 with right hemianopia following a scan of approximately 15°. Data are plotted from the time at which the pedestrian appeared (0 seconds) to the time at which it disappeared. The eccentricity of the stationary pedestrians in plots (a–c) increased rapidly as the car advanced while the eccentricity of the approaching pedestrians in plots (d, e) remained approximately constant for more than 4 seconds. A 0° gaze angle means that the participant was looking along the car heading direction, which was essentially straight ahead because the pedestrian events occurred on straight road segments.

Approaching pedestrians always stopped before entering the participant's lane to avoid collisions; however, they were programmed to run at such speed that if the car had continued at the posted speed limit and the pedestrian had not stopped before the travel lane, a collision would have occurred. The eccentricity of stationary pedestrians with respect to the car heading increased rapidly (Figs. 1a–c). By compari-

son, the eccentricity of the approaching pedestrians was approximately constant for at least 3 seconds after appearance (Figs. 1d, 1e), providing the car was driven within ±10 mph of the speed limit.

Participants were instructed to obey all the normal rules of the road, maintain the posted speed and to press the large horn (in the center of the steering wheel) whenever they saw a pedestrian figure. They were told that pedestrians could appear on either side of the road but were not given specific information about pedestrian eccentricities or numbers. Moreover, they were not given any instructions about scanning or the use of specific scanning strategies to look for pedestrians, and they were not given any feedback about their detection performance during the driving simulator sessions

Detection rates, reaction times, and the proportion of timely responses for the small and large eccentricity pedestrians were previously reported in detail.[5] In this paper, we focus on an analysis of gaze scan magnitudes.

Gaze and Pedestrian Eccentricity on the Blind Side

Gaze and pedestrian eccentricities (in the horizontal plane) were calculated with respect to the car heading direction for all pedestrians that appeared at approximately 14° on the blind side (Fig. 1). Data from small (~4°) eccentricity blind-side pedestrians were not included in the analysis because it was sometimes impossible to reliably distinguish small magnitude saccades (≤4°) from noise in the recorded gaze data. Only gaze movements that took the eyes at least 6° into the blind hemifield, and could therefore be analyzed with little ambiguity, were included in analyses. A gaze scan was defined as a movement (the combined head + eye movement) taking the eye from the straight ahead gaze position into the blind hemifield that had a magnitude of at least 6°. Movements that returned the eyes from the blind hemifield toward the straight-ahead gaze position were categorized as return movements, not scans, and were not analyzed.

For each pedestrian appearing at approximately 14° on the blind side, gaze scans toward the blind hemifield were analyzed from the time at which the pedestrian appeared to the time of the horn press (logged electronically by the driving simulator) when pedestrians were detected, or to the time at which the pedestrian disappeared when pedestrians were not detected. Gaze scans toward the blind hemifield comprised either a single movement (e.g., scans at ~4 and 5 seconds in Fig. 1d) or a series of sequential saccades in a stepwise manner (Figs. 1a, 1b). The gaze scan was always defined as the whole movement, from straight ahead to the maximum eccentricity into the blind hemifield. Each scan was quantified in terms of the magnitude (the maximum eccentricity into the blind hemifield) and the time after the pedestrian appearance at which the scan reached the maximum eccentricity. When detection occurred participants had a strong tendency to keep fixating the pedestrian or to make several scans back to the pedestrian (Figs. 1a, 1b, and 1d). To address our main hypotheses, we were only interested in analyzing scanning behaviors until the point of detection; therefore, gaze scans after the horn press were not analyzed.

Each gaze scan was also categorized by whether or not it reached the pedestrian. A scan was classified as having reached the pedestrian if gaze intersected the pedestrian or came within 2° of the pedestrian (as the accuracy of the gaze tracker was 2° across the central screen where the pedestrians appeared). When a pedestrian was detected, the first scan to reach the pedestrian before the horn press, as well as any earlier scans that did not reach the pedestrian, were included in analyses. When a pedestrian was missed, all scans that did not reach the pedestrian from the time of appearance to disappearance were included.

In addition, when a gaze scan intersected with the pedestrian (or came within 2° of the pedestrian), we determined the time after the pedestrian appearance of the first intersection (or when the scan came within 2°) and the eccentricity of the pedestrian at that time point.

For the 14° eccentricity pedestrians on the blind side, there were 13 events in the approaching condition and 13 in the stationary condition for each subject, giving a total of 312 events across the 12 participants. Due to technical difficulties, gaze data were not available for 12 of these events. Of the remaining 300 events, 21 (7%) were excluded from analysis for the following reasons: too much missing gaze data ($n = 11$); gaze data were too noisy ($n = 9$); and the driver stopped the car abruptly during a pedestrian event ($n = 1$). Thus, a total of 279 events were included in analyses.

Gaze and Pedestrian Eccentricity on the Seeing Side

For comparison purposes, gaze and pedestrian eccentricities (in the horizontal plane) were also

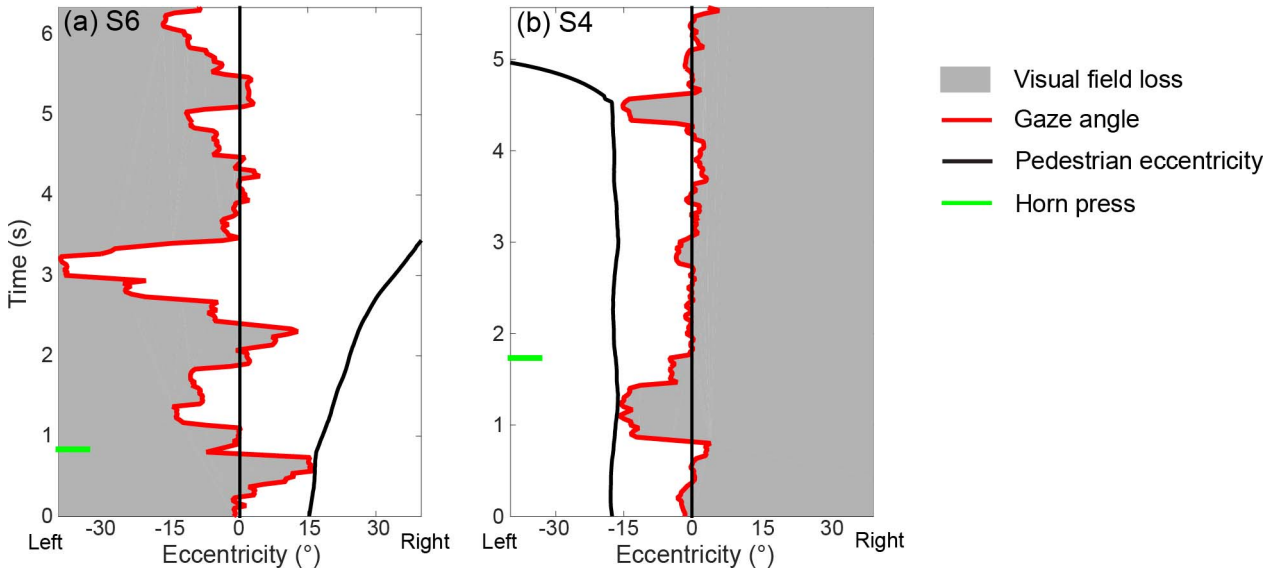

Figure 2. Plots for individual participants of lateral gaze eccentricity (*thick red line*) and pedestrian eccentricity (*thick black line*) with respect to car heading direction for pedestrians initially appearing at approximately 14° in the seeing hemifield: (a) a stationary pedestrian detected by participant S6; and (b) an approaching pedestrian detected by participant S4. In both cases there was a gaze scan to the pedestrian within 1 second of the pedestrian appearance (although S6 made a faster horn-press response). Data are plotted from the time at which the pedestrian appeared (0 seconds) to the time at which it disappeared.

calculated with respect to the car heading direction for all pedestrians that appeared at approximately 14° on the seeing side. Again, a gaze scan was defined as a movement (the combined head + eye movement) taking the eye from the straight ahead gaze position into the seeing hemifield that had a magnitude of at least 6°. As detection rates were 100% for pedestrians on the seeing side, gaze scans toward the seeing hemifield were only analyzed from the time at which the pedestrian appeared to the time of the horn press (Fig. 2).

For the 14° eccentricity pedestrians on the seeing side, there were 13 events in the approaching condition and 13 in the stationary condition for each subject, giving a total of 312 events across the 12 participants. Due to technical difficulties, gaze data were not available for 13 of these events; thus, a total of 299 events were included in analyses.

Statistical Analyses

Two-sample Kolmogorov-Smirnov tests were used to test for differences between the stationary and approaching conditions in the distributions of scan magnitudes and in the distributions of times at which scans were made. In addition, median scan magnitudes were computed for each participant. Differences in median scan magnitudes between the two conditions and between the first and last two drives in each condition were analyzed with nonparametric tests. Statistical analyses were performed with STATA version 14.2 (StataCorp, College Station, TX) with an alpha level of 0.05 for all analyses.

Results

Participant Characteristics

Participants varied widely in terms of age, time since onset of the lesion, and driving experience (Table 1), representing the wide variability that can be expected in a clinical population. Stroke was the main cause of the HH. Two of the 12 participants were current drivers. Eight had stopped driving following the onset of the HH and had last driven a median of 2 years (range, 0.5–6) before participating in the study. The remaining two had never obtained a driving license, but had been driving regularly off-road on private land for at least 1 year. Two participants had hemiparesis (1 right and 1 left), but were able to steer the vehicle and press the large horn (in the center of the steering wheel) without any difficulties.

Detection Performance Summary

There were a significantly higher proportion of detected pedestrians on the blind side in the approaching than the stationary condition (69% vs.

Table. Characteristics of the 12 Study Participants

Subject	Sex	Age, y	Side of HH	Years Since Onset	Cause	Hemiparesis	Age When Licensed, y	Current Driver	Years Since Stopped
S1	Female	47	Right	8	Stroke	No	16	Yes	N/A
S2	Female	36	Right	5	Stroke	No	16	No	5
S3	Male	57	Left	4	Stroke	No	16	No	3
S4	Male	45	Right	5	Trauma	No	16	No	4
S5*	Male	34	Left	19	Tumor	No	-	Off-road†	N/A
S6	Male	18	Left	12	Tumor	No	17	Yes	N/A
S7	Male	43	Left	0.5	Tumor	No	16	No	0.5
S8*	Female	31	Right	31	Stroke	Yes	17	No	6
S9*	Male	33	Right	1	Stroke	No	18	No	1
S10	Female	28	Left	2	Stroke	Yes	16	No	1
S11	Male	18	Left	1	Stroke	No	-	Off-road†	N/A
S12	Female	82	Right	2	Stroke	No	16	No	1
Median		35		4.5			16		2

N/A, not applicable.

* S5, S8, and S9 showed evidence of adapting their scan magnitudes.

† S5 and S11 did not hold a driving license but drove regularly off-road on private land.

51%; $P = 0.002$) and response times were significantly longer (medians 2.9 vs. 1.7 seconds, $P = 0.02$). By comparison, detection rates and response times on the seeing side did not differ between the two conditions (100% vs. 100%, and 1.2 vs. 1.2 seconds, respectively).

Sample Plots of Pedestrian and Gaze Eccentricity

Figure 1 presents individual plots of lateral gaze and pedestrian eccentricity with respect to car heading direction for five events in which pedestrians initially appeared at approximately 14° on the blind side. For comparison, Figure 2 presents individual plots for two events in which pedestrians initially appeared at approximately 14° on the seeing side. Data are plotted from the time the pedestrian appeared to the time it disappeared.

Figure 1a provides an example of an early detection of a stationary pedestrian on the blind side by participant S6. A gaze scan of approximately 13° first reached the pedestrian at 0.35 seconds, when detection likely occurred, and the pedestrian was then fixated. The horn press to confirm detection occurred shortly afterwards at 0.9 seconds (short green line). Figure 1b provides an example of a later detection of a stationary blind-side pedestrian by the same participant (S6). The gaze scan needed for detection was much larger (~28°) and reached the pedestrian about 3 seconds after it appeared. Figure 1c provides an example of a failure to detect a blind-side stationary pedestrian by participant S9. Although a gaze scan reached 20° eccentricity about 2.8 seconds after the pedestrian appeared, it did not reach as far as the pedestrian, which was at 26° eccentricity. Figure 1d provides an example of an early detection by S6 of an approaching blind-side pedestrian with a gaze scan of 15° about 1 second after the pedestrian appeared. Interestingly, after fixating the pedestrian for almost 1 second, S6 made another gaze movement further into the blind hemifield. Figure 1e provides an example of a very late detection of an approaching blind-side pedestrian. Participant S4 detected the pedestrian with a gaze scan of 15° about 4.7 seconds after it appeared. By comparison, in Figure 2, participants S6 and S4 both made a gaze scan to a pedestrian on the seeing side less than 1 second after it appeared. This was the case for the majority of pedestrian events on the seeing side.

Eccentricity and Time When Gaze First Reached the Pedestrian on the Blind and Seeing Sides

Figure 3 shows pedestrian eccentricity at the time when gaze first reached (intersected) the pedestrian for all blind-side and seeing-side pedestrians that were detected. For clarity, data were grouped in four time bins after the pedestrian appearance. As expected, the

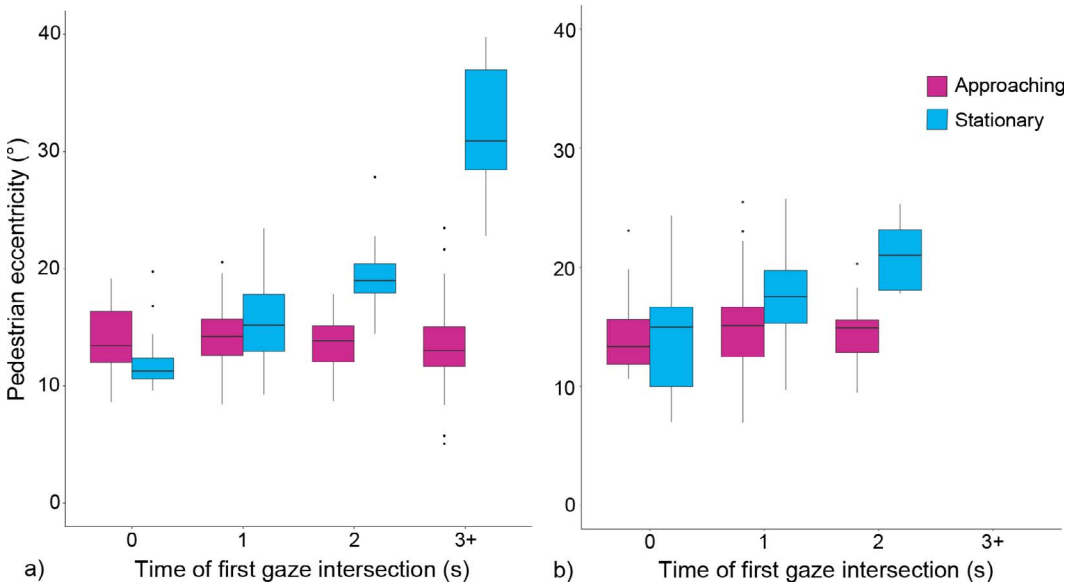

Figure 3. Boxplots of pedestrian eccentricity at the time of first gaze intersection for all pedestrians that were detected after appearing on (a) the blind side and (b) the seeing side (data pooled across all participants). Pedestrian eccentricity remained approximately constant in the approaching condition but increased rapidly in the stationary condition with increasing time after the pedestrian appearance. Data are grouped in four time bins (Bin 0: <0.5 seconds; Bin 1: 0.5–1.4 seconds; Bin 2: 1.5–2.4 seconds; Bin 3+: ≥2.5 seconds). The *thick line* in box center represents the median; box length represents the IQR; *whiskers* represent data within 1.5 times IQR; *dots* are outlier data points beyond 1.5 times IQR.

pedestrian eccentricity remained fairly constant with medians ranging from 13° to 15° in the approaching condition, but increased rapidly in the stationary condition, from a median of 11° in the first time bin to 31° in the last time bin (≥2.5 seconds) on the blind side (Fig. 3a). The range of eccentricities within each bin, even in the first time bin, reflects variations in participants' vehicle speed and lane position across events, which in turn affected the measured pedestrian eccentricity. Within each time bin, the eccentricities at which gaze first reached the pedestrian did not differ on the blind and seeing sides. Rather, the main difference between the two sides was in the distribution of the timing of the first scan to reach the pedestrian (Fig. 4). On the blind side, the first scan to reach the pedestrian occurred later, on average, than on the seeing side (medians of 1.25 and 0.75 seconds, respectively). On the blind side only approximately 40% of scans to reach the pedestrian were made within 1 second of the pedestrian appearing compared with approximately 70% on the seeing side (Fig. 4).

Did Participants Adapt Their Blind-Side Gaze Scan Magnitudes?

Contrary to our prediction, the overall distributions of blind-side gaze scan magnitudes did not differ between the approaching and stationary conditions (two-sample Kolmogorov-Smirnov test, $P = 0.25$; Fig. 5). Furthermore, median scan magnitudes (per participant) did not differ between the two conditions (overall medians (IQR): approaching 14° (9°–15°) and stationary 13° (9°–20°); $n = 12$, $z = 0.78$, $P = 0.43$). Thus, our results suggest that, on average, the participants did not make larger scans to the blind side in the stationary condition (the majority of data points are close to the diagonal in Fig. 6). There was, however, one participant (S5) with a noticeably larger median scan magnitude in the stationary than the approaching condition (35° and 14°, respectively; solid square well below the diagonal in Fig. 6), suggesting that he did adapt his scan magnitudes. There was also one participant, S9, who made noticeably smaller scans in the stationary than the approaching condition (medians 21° and 32°, respectively; solid triangle well above the diagonal in Fig. 6); we discuss possible interpretation of this in the next section. When the median scan magnitudes were compared for sessions 1 and 2 (rather than stationary and approaching) no significant differences were found between the two sessions ($P = 0.99$). Thus, there was no overall between-session learning effect with larger magnitudes at the second session, irre-

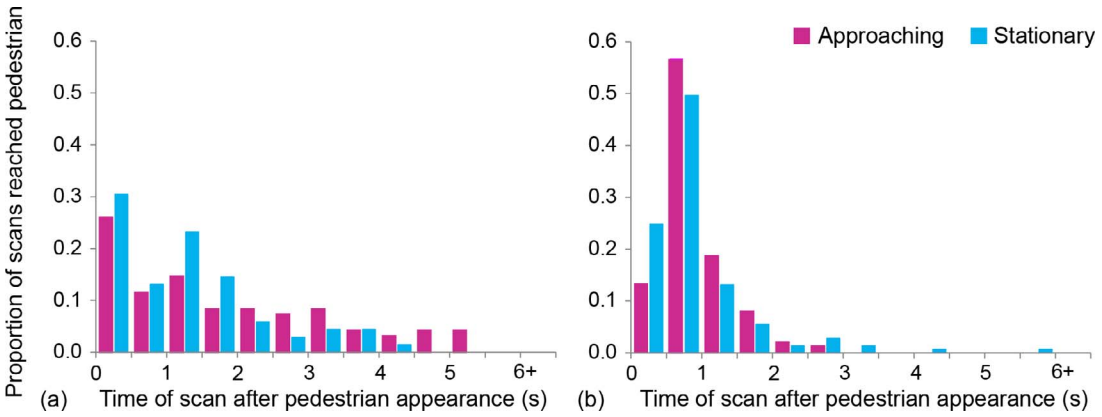

Figure 4. Frequency histograms of the time after the pedestrian appearance at which scans were made on (a) the blind side and (b) the seeing side for the first scan to reach the pedestrian.

spective of whether the second session was the approaching or stationary condition.

To further investigate learning effects, we compared median blind-side scan magnitudes for each participant in the first two drives and the last two drives in each condition (Fig. 7). Median scan magnitudes did not differ between the first two and last two drives for the approaching condition ($n = 10$, $z = 0.663$, $P = 0.51$; equal number of data points above and below the diagonal in Fig. 7). However, there was a trend for median scan magnitudes to be larger in the last two drives than the first two drives in the stationary condition ($n = 11$, $z = 1.78$, $P = 0.08$; more data points above than below the diagonal in Fig. 7).

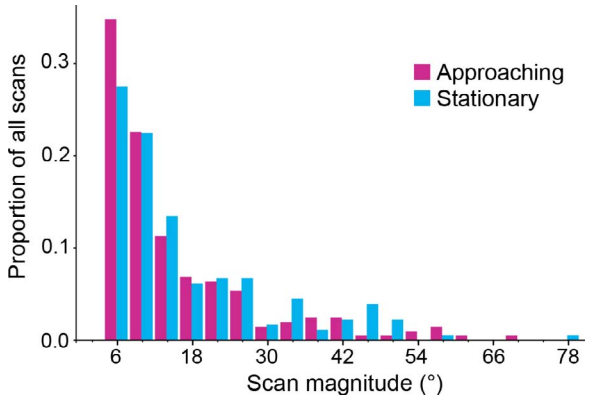

Figure 5. Frequency histogram of scan magnitudes for approaching and stationary pedestrians for gaze scans to the blind side (including scans that reached and did not reach the pedestrian). The distributions did not differ between the two conditions ($P = 0.25$). Each bin width is 4°. Only scans >6° were included in analyses.

Participants Who Showed Evidence of Adaptive Behaviors

There were only three participants (S5, S8, and S9) who showed evidence of within-session learning effects in scan magnitudes to the blind side. The adaptive behavior of each is considered in detail in the following paragraphs. They were all in the 30- to 35-year age range, but differed widely in the time since the onset of the HH and only S5 was currently driving (Table 1).

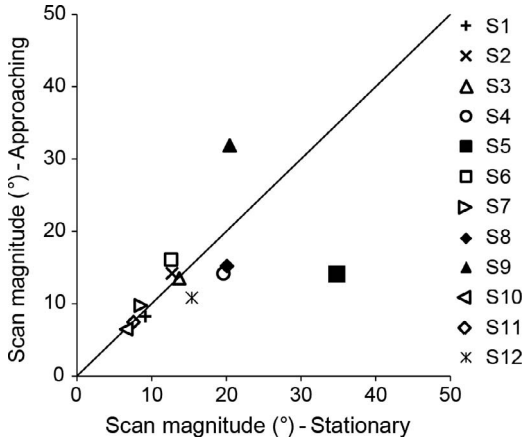

Figure 6. Scatterplot showing median blind-side scan magnitudes for each participant for the approaching and stationary conditions. For the majority of participants scan magnitudes did not differ in the two conditions (points close to the diagonal). However, participant S5 had larger scan magnitudes in the stationary condition than the approaching condition (*solid square* well below the diagonal) while participant S9 had larger scan magnitudes in the approaching condition (*solid triangle* above the diagonal). Data are pooled across scans that reached and did not reach the pedestrian.

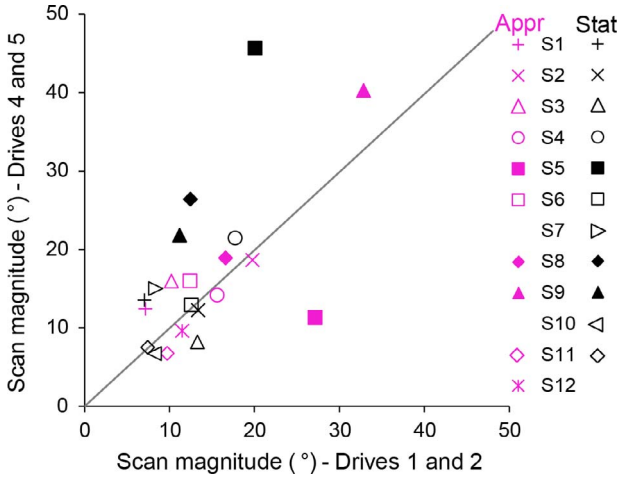

Figure 7. Scatterplot showing median blind-side scan magnitudes for each participant for the last two drives and the first two drives in the approaching (*pink symbols*) and stationary (*black symbols*) conditions. There was no increase in scan magnitudes between the first two and last two drives for the approaching condition (approximately equal numbers of *pink symbols* above and below the diagonal). However, three participants S5, S8, and S9 (*solid filled symbols*) showed evidence of adaptive behaviors in the stationary condition having larger scan magnitudes for the last two than the first two drives (*solid black symbols* well above the diagonal). Participant S5 also showed adaptive behavior in the approaching condition having larger scans in the first two than the last two drives (*solid pink square* well below the diagonal). Data are pooled across scans that reached and did not reach the pedestrian. Data are missing for participants S7 and S10 in the approaching condition and S12 in the stationary condition because they did not make any scans >6° in the segments with 14° blind-side pedestrians in drives 4 and 5 in those conditions.

Participant S5 showed within-session adaptive behaviors in both the approaching condition (the first simulator session for S5) and the stationary condition (the second simulator session for S5). In the approaching condition (pink filled square in Fig. 7), scan magnitudes decreased from 27° to 11°, respectively, suggesting that he learned he could detect the approaching pedestrians with smaller magnitude scans. In the stationary condition (black filled square in Fig. 7), his scan magnitudes increased from 20° in the first two drives to 46° in the last two drives of that session (suggesting he learned that he needed to make larger scans to detect the stationary pedestrians where eccentricity increased rapidly after the pedestrian appeared).

Participant S8 also showed within-session learning. Scan magnitudes increased from median 13° in the first two drives to 26° in the last two drives in the stationary condition, which was the first simulator session for S8 (black filled diamond in Fig. 7). By comparison, in the approaching condition at the second session for S8, there was little change in scan magnitudes (medians 17° and 19°, respectively; pink filled diamond in Fig. 7). This was possibly because she realized that her scan magnitudes were sufficient to detect the approaching pedestrians, which maintained a median eccentricity around 14°.

Participant S9 appeared to show learning effects in the stationary condition (the second simulator session for S9) with scan magnitudes increasing from median 11° in the first two drives to 22° in the last two drives (black filled triangle in Fig. 7). Scan magnitudes also increased a little in the approaching condition (the first driving simulator session for S9) from 33° to 40° (pink filled triangle in Fig. 7); however, those magnitudes were much greater than needed to detect the approaching pedestrians. The more noticeable change in scan magnitudes for this participant was between the last two drives of the first session (approaching condition) and the first two drives of the second session (stationary condition), medians 40° and 11°, respectively. These data possibly suggest he realized at the end of the first session that he did not need to make such large scans to detect the approaching pedestrians and reduced his scan magnitudes at the start of the second session, only to find that they were insufficient to detect the stationary pedestrians with a consequent increase in scan magnitudes to 22° by the end of that session. However, we did not debrief our participants about their strategies and they did not volunteer any comments about such a strategic approach.

Magnitudes of Blind-Side Scans That Reached and Did Not Reach the Pedestrian

To address whether differences in detection rates were related to differences in scanning requirements, we compared scan magnitudes for scans that reached (detection occurred) and did not reach (detection did not occur) blind-side pedestrians for the approaching and stationary conditions. As expected, blind-side scans that reached the pedestrian were of a greater magnitude than scans that did not reach the pedestrian (overall medians 23° vs. 10°; $n = 10$, $z = 2.80$, $P = 0.005$), and this was true for both the approaching condition (20° vs. 8°; $n = 10$, $z = 2.80$, $P = 0.005$) and the stationary condition (26° vs. 11°, $n = 10$, $z = 2.19$, $P = 0.029$). Figure 8 shows median magnitudes for scans that reached and did not reach the pedestrian as a function of time after the

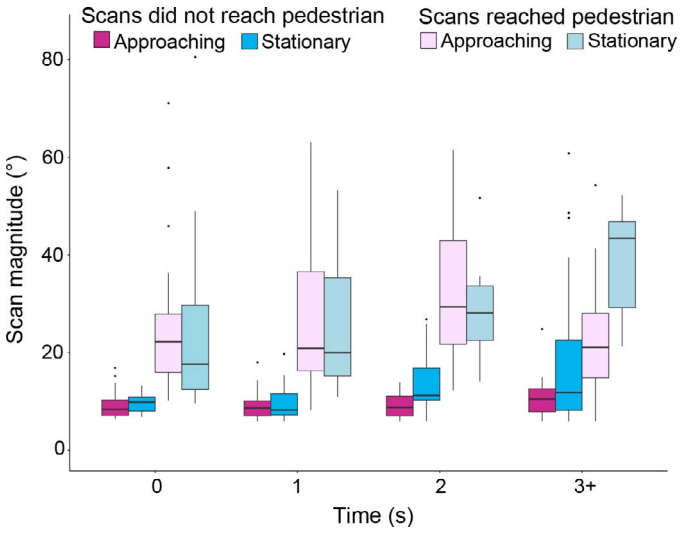

Figure 8. Boxplots of blind-side scan magnitudes for approaching and stationary pedestrians for scans that reached (detection occurred) and did not reach (detection did not occur) the pedestrian (data pooled across all participants). In the last time bin, the magnitudes of scans that reached and also did not reach the pedestrian were larger in the approaching than the approaching condition reflecting the much greater pedestrian eccentricity in the stationary than the approaching condition at this time point (see the last time bin in Fig. 3). Data are grouped in four time bins (Bin 0: <0.5 seconds; Bin 1: 0.5–1.4 seconds; Bin 2: 1.5–2.4 seconds; Bin 3+: ≥2.5 seconds).

pedestrian appearance for the two conditions; scans are grouped in four time bins for clarity. In the first two bins (up to 1.4 seconds), the distributions of the reached and nonreached scans did not differ in the two conditions (all $P > 0.56$). In the third time bin (1.5–2.4 seconds), the distributions of the reached scans did not differ in the two conditions ($P = 0.34$), but the distributions of the nonreached scans did differ ($P = 0.012$) with more scans of larger magnitude in the stationary condition. In the fourth time bin (≥2.5 seconds), there were more scans of larger magnitude in the stationary than the approaching condition for scans that both reached and did not reach the pedestrian ($P = 0.009$ and 0.08, respectively). The differences between the two conditions were especially noticeable for scans that reached the pedestrian (detection occurred) with medians of 42° and 21°, respectively (Fig. 8). These observations are consistent with the large difference in pedestrian eccentricities between the two conditions in the fourth time bin (median eccentricity 31° in the stationary condition compared with 13° in the approaching condition; Fig. 3a). Thus, in the fourth time bin very large scans were needed for detection to occur in the stationary condition while detection was still possible in the approaching condition with more moderate sized scans of the same magnitude as in the first time bin.

Was More Time Available for Blind-Side Scans to Reach Approaching Pedestrians?

The overall distributions of the times at which scans were made after the pedestrian appearance did not differ between the approaching and stationary conditions ($P = 0.16$). However, when scans that reached (detection occurred) and did not reach (detection did not occur) the pedestrian were considered separately, then significant differences were found between the two conditions. Consistent with our hypothesis, a higher proportion of scans that reached the pedestrian occurred at later times in the approaching than the stationary condition ($P = 0.03$; Fig. 9a). By comparison, a higher proportion of the scans that did not reach the pedestrian occurred at later times in the stationary than the approaching condition ($P = 0.001$; Fig. 9b). For example, 31% of scans that reached the pedestrian did so after 2.5 seconds in the approaching condition compared with only 13% in the stationary condition. As a consquence, there was a correspondingly higher proportion of pedestrians detected after 2.5 seconds in the approaching than the stationary condition.

Discussion

Although people with HH might be able to use voluntary, cognitive control to guide blind-side scanning, little is known about the extent to which they are able to do so in real-world situations. Using the controlled setting of a driving simulator, we examined whether people with HH were able to spontaneously adapt their blind-side scan magnitudes in response to differing scanning requirements for detection of pedestrians when differing cues about pedestrian eccentricities and movement behaviors were available in the seeing hemifield. The pedestrians either walked/ran toward the driving lane on a collision course with the participant's car or stood stationary to the side of the lane. We did not give any instructions or training in how to scan to look for the pedestrians while driving because our goal was to evaluate spontaneous adaptation.

The two conditions presented different scanning requirements for successful detection of pedestrians appearing in the blind hemifield. While the eccentric-

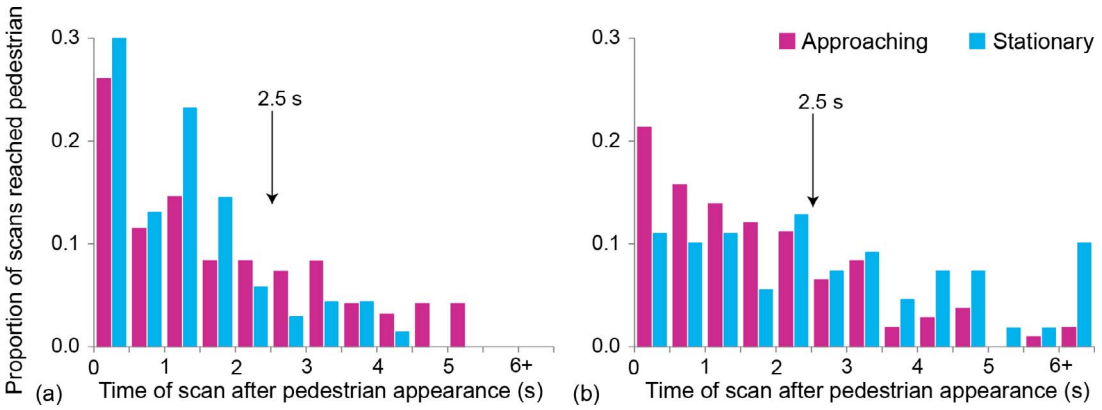

Figure 9. Frequency histogram of the time after the pedestrian appearance at which blind-side scans were made, which (a) reached the pedestrian and (b) did not reach the pedestrian. Scans that occurred late after the pedestrian appearance (after 2.5 seconds) were more likely to (a) reach the pedestrian in the approaching than the stationary condition and (b) conversely more likely to fail to reach the pedestrian in the stationary than the approaching condition. (Note: Fig. 9a is the same as Fig. 4a, but plotted here with a different range on the y-axis to facilitate direct comparison with Fig. 9b).

ity of the stationary pedestrians increased rapidly with a median of 31° after 2.5 seconds, requiring increasingly larger scans for detection, the eccentricity of the approaching pedestrians remained approximately constant at median 14° even after 2.5 seconds (Fig. 3), requiring a more moderate sized scan for detection. However, even a moderate scan of 14° is close to the limit of a typical eye saccade; eye saccades of normally-sighted observers when walking are usually less than 15°.[18,19] Thus, the appearance eccentricity of 14° presented a challenging situation in terms of the scanning demands for participants with complete HH. Head as well as eye movements were often needed to scan sufficiently far into the blind hemifield, especially in the stationary condition.

There were clear differences in scanning behaviors toward pedestrians appearing in the blind and seeing hemifields (compare Figs. 1 and 2). When a pedestrian appeared in the seeing hemifield, there was typically a single gaze scan to the pedestrian, which occurred within 1 second of the appearance. By comparison, the timing of the first scan to reach a pedestrian in the blind hemifield was much more variable reflecting the lack of both temporal and eccentricity-related visual cues from peripheral vision on that side. When a pedestrian was present in the blind hemifield, it was by chance whether a scan to the blind side was made. Interestingly participants did not rely entirely on peripheral vision for detection of pedestrians in the seeing hemifield. In the vast majority of cases, they fixated the pedestrian before pressing the horn.

Given that participants were all aware of their hemifield loss and information about the eccentricity and relative movement of pedestrians was readily available on the seeing side, we evaluated the extent to which they modified the magnitudes of their blind-side gaze scans to match the differing pedestrian eccentricities in the two conditions. Contrary to our hypothesis that blind-side scans would, on average, be larger in the stationary than the approaching condition, the overall distributions of scans magnitudes did not differ in the two conditions (Fig. 5). There was only one participant, S5, who made larger blind-side scans in the stationary than the approaching condition. Interestingly, the median magnitudes of those scans (35° and 14°, respectively) were very close to the median pedestrian eccentricities in the two conditions after 2.5 seconds (31° and 14°, respectively).

If participants had used information from the seeing side to guide their blind-side scanning, then we would have expected to find evidence of within session changes in scan magnitudes. Of the 12 participants, three did demonstrate evidence of within session adaptation of their blind-side scan magnitudes to match the differing pedestrian eccentricities in the two conditions. Participant S5, who drove regularly on private land, exhibited adaptive behaviors in both the stationary and approaching conditions, increasing scan magnitudes in the former and decreasing scan magnitudes in the latter. Participants S8 and S9, both former drivers, also showed learning effects in the stationary condition with median scan magnitudes increasing between the first and last two drives. However, the two participants S1 and S2, who were current on-road drivers

did not exhibit any evidence of adaptive behaviors. Interestingly, Nowakowska et al.[20] also reported that a similar proportion of participants (4/20) with simulated HH modified their search strategy in response to differing task demands, starting search from the blind side rather than the seeing side when the search task was easy and the target could be easily detected in peripheral vision. As in the current study, participants were not given any instructions about specific scanning strategies and did not receive any training other than practice trials.

The second question we examined in this paper was whether differences in detection performance between the stationary and approaching condition were accounted for by the differences in the scanning requirements of the two conditions. Detection rates were higher and response times were longer for the approaching than the stationary condition. Up to 1.5 seconds after the pedestrian appearance, there was little or no difference between the two conditions in terms of the magnitudes of scans that reached the pedestrian (Fig. 8). It was only at later times, especially beyond 2.5 seconds after the pedestrian appearance, that differences emerged. At these later times significantly larger scan magnitudes were needed for detection in the stationary (median 31°) than the approaching condition (median 14°) because the pedestrian eccentricity was much greater. As a consequence, relatively few scans reached the pedestrian after 2.5 seconds in the stationary condition. By comparison, in the approaching condition, an approximately 14° scan was still sufficient to reach the pedestrian after 2.5 seconds, and in some cases almost up until the time that it disappeared (Fig. 1e). Approximately 31% of scans that reached the pedestrian occured after 2.5 seconds in the approaching condition (compared with only 13% in the stationary condition), resulting in overall higher detection rates but longer response times.

Thus, differences in the scanning requirements did account for the differences in detection performance between the two conditions. Stationary pedestrians were more likely to be missed because there was only a small time window within which an approximately 14° gaze scan would be large enough to reach the pedestrian eccentricity. The more safety-relevant approaching pedestrians stayed at a fixed eccentricity for longer allowing more time for a typical (moderate) scan to reach them resulting in better detection rates. However, the magnitude of gaze scanning to the blind side was still often insufficient and the majority of participants still had blind-side detection deficits (missed detections or delayed responses) that could potentially result in a collision in real-world driving.

To compensate effectively in everyday life, it seems that patients with HH would need to be able to adapt their scanning strategy to the demands of differing enviroments and situations, requiring voluntary, cognitive control of blind-side scanning. Based on their studies with simulated HH, Schuett et al.[13] advocated task-specific scanning training for patients with HH, while Nowakowska et al.[20] suggested that patients should be trained to rapidly adjust their search strategy depending on the particular visual context (e.g., searching for a small object in a cluttered environment versus a large object in an uncluttered environment). However, the results of our study indicate that a majority of people with long-standing HH do not seem to be able to rapidly and spontaneously modify their scanning strategy, even in the presence of clear cues from the seeing side. If they were unable to adapt their scanning in conditions where the frequency and position of pedestrians were far more predictable than in real-world driving, then it seems unlikely that they would be able to adapt to rapidly changing and unpredictable situations in on-road driving.

In summary, our results suggest that 25% of participants (3/12) were able to use voluntary, cognitive control to modify their blind-side scan magnitudes to match the differing scanning requirements of the two pedestrian conditions without any specific instructions or training. It is possible that some of the participants may have exhibited other changes in scanning behaviors that our analysis did not capture. We expect that more participants would have modified their scan magnitudes if explicit training had been given. Our goal, however, was to evaluate spontaneous adaptation of scanning behaviors; therefore, explicit training was not given. More research is needed to establish the extent to which people with HH use effective scanning strategies in real-world mobility situations, whether they are able to adapt their scanning strategies in response to differing task demands, and whether scanning training generalizes to everyday mobility tasks. Each of these topics needs to be addressed using objective recordings of gaze behaviors,[21] which is challenging in uncontrolled, dynamic mobility situations, especially when walking. Driving simulators can provide a safe, controlled, and repeatable test environment for such studies.

Acknowledgements

Supported in part by National Institutes of Health Grants: R01-EY025677 (AB), R00-EY018680 (AB), K99-EY026130 (CA), R01-EY12890 (EP) and S10-RR028122 (EP).

Disclosure: **C.F. Alberti**, None; **R.B. Goldstein**, None; **E. Peli**, None; **A.R. Bowers**, None

References

1. Zhang X, Kedar S, Lynn MJ, Newman NJ, Biousse V. Homonymous hemianopias - clinical-anatomic correlations in 904 cases. *Neurology*. 2006;66:906–910.
2. Bowers AR. Driving with homonymous visual field loss: a review of the literature *Clin Exp Optometry*. 2016;99:402–418.
3. Bowers AR, Mandel AJ, Goldstein RB, Peli E. Driving with hemianopia: I. Detection performance in a simulator. *Invest Ophthalmol Vis Sci*. 2009;50:5137–5147.
4. Papageorgiou E, Hardiess G, Ackermann H, et al. Collision avoidance in persons with homonymous visual field defects under virtual reality conditions. *Vision Res*. 2012;52:20–30.
5. Alberti CF, Peli E, Bowers AR. Driving with hemianopia: III. Detection of stationary and approaching pedestrians in a simulator. *Invest Ophthalmol Vis Sci*. 2014;55:368–374.
6. Bowers AR, Ananev E, Mandel AJ, Goldstein RB, Peli E. Driving with hemianopia: IV. Head scanning and detection at intersections in a simulator. *Invest Ophthalmol Vis Sci*. 2014;55:1540–1548.
7. Bahnemann M, Hamel J, de Beukelaer S, et al. Compensatory eye and head movements of patients with homonymous hemianopia in the naturalistic setting of a driving simulation. *J Neurol*. 2015;262:316–325.
8. Smith M, Mole CD, Kountouriotis GK, Chisholm C, Bhakta B, Wilkie RM. Driving with homonymous visual field loss: does visual search performance predict hazard detection? *Br J Occup Ther*. 2015;78:85–95.
9. Bowers AR, Tant M, Peli E. A pilot evaluation of on-road detection performance by drivers with hemianopia using oblique peripheral prisms *Stroke Res Treat*. 2012;2012:176806
10. Iorizzo DB, Riley ME, Hayhoe M, Huxlin KR. Differential impact of partial cortical blindness on gaze strategies when sitting and walking - an immersive virtual reality study. *Vision Res*. 2011;51:1173–1184.
11. de Haan GA, Melis-Dankers BJM, Brouwer WH, Tucha O, Heutink J. The effects of compensatory scanning training on mobility in patients with homonymous visual field defects: a randomized controlled trial. *PLoS One*. 2015;10:e0134459.
12. Schuett S, Kentridge RW, Zihl J, Heywood CA. Are hemianopic reading and visual exploration impairments visually elicited? New insights from eye movements in simulated hemianopia. *Neuropsychologia*. 2009;47:733–746.
13. Schuett S, Heywood CA, Kentridge RW, Dauner R, Zihl J. Rehabilitation of reading and visual exploration in visual field disorders: transfer or specificity? *Brain*. 2012;135:912–921.
14. Bronstad PM, Bowers AR, Albu A, Goldstein RB, Peli E. Driving with central field loss I: effect of central scotomas on responses to hazards. *JAMA Ophthalmol*. 2013;131:303–309.
15. Vanier M, Gauthier L, Lambert J, et al. Evaluation of left visuospatial neglect: norms and discrimination power of two tests. *Neuropsychology*. 1990;4:87–96.
16. Schenkenberg T, Bradford DC, Ajax ET. Line bisection and unilateral visual neglect in patients with neurologic impairment. *Neurology*. 1980;30:509–517.
17. Folstein MF, Folstein SE, McHugh PR. Mini-mental state. A practical method for grading the cognitive state of patients for the clinician. *J Psychiatr Res*. 1975;12:189–198.
18. Bahill AT, Adler D, Stark L. Most naturally occurring human saccades have magnitudes of 15 degrees or less. *Invest Ophthalmol*. 1975;14:468–469.
19. Luo G, Vargas Martin F, Peli E. The role of peripheral vision in saccade planning: learning from people with tunnel vision. *J Vis*. 2008;8(14):25.
20. Nowakowska A, Clarke ADF, Sahraie A, Hunt AR. Inefficient search strategies in simulated hemianopia. *J Exp Psychol Hum Percept Perform*. 2016;42:1858–1872.
21. Tomasi M, Pundlik S, Bowers AR, Peli E, Luo G. Mobile gaze tracking system for outdoor walking behavioral studies. *J Vis*. 2016;16(3):27.